Supporting information to

Charge Clamps of Lysines and Hydrogen Bonds Play Key Roles in the Mechanism to Fix Helix 12 in the Agonist and Antagonist Positions of Estrogen Receptor α: Intramolecular Interactions Studied by the *Ab Initio* Fragment Molecular Orbital Method

Chiduru Watanabe,[*,†,⊥] Kaori Fukuzawa,[‡,§] Shigenori Tanaka,[‖]

and Sachiko Aida-Hyugaji[†]

[†] Information and Communication Technology Education Center, Tokai University, 4-1-1 Kitakaname, Hiratsuka, Kanagawa 259-1292, Japan

[‡] Mizuho Information & Research Institute, Inc., 2-3 Kanda Nishiki-cho, Chiyoda-ku, Tokyo 101-8443, Japan

[§] Institute of Industrial Science, The University of Tokyo, 4-6-1 Komaba, Meguro-ku, Tokyo 153-8505, Japan

[‖] Graduate School of System Informatics, Department of Computational Science, Kobe University, 1-1 Rokkodai, Nada-ku, Kobe, Hyōgo 657-8501, Japan

Corresponding Author

[*]chiduru.watanabe@riken.jp (Chiduru Watanabe)

Present Address

[⊥]RIKEN Center for Life Science Technologies, Drug Discovery Computational Chemistry Platform Unit, 1-7-22 Suehiro-cho, Tsurumi-ku, Yokohama City, Kanagawa, 230-0045, Japan.

A. Solvent and Screening Effects

In our article, we have shown that certain residues play a key role in the determination of the H12 position. However, such roles of the key residues may not perfectly represent the biological reality, because the X-ray structure under crystalline condition and the biomolecular structure under physiological condition are obtained under different conditions (e.g., with or without solvent water). Therefore, we have examined solvent and screening effect for intra-molecular interactions by using explicit and implicit water models.

Computational Method for Explicitly Solvated Water Model.

The explicit water model is generated by the molecular dynamics (MD) simulation as follows. We employed Amber 10 package with the AMBER99SB force field and the gaff, the general AMBER force field (in the Supporting Information, Sec. A and B) for the structural optimization and the MD simulation, where the periodic boundary condition with explicit water (the TIP3P water surrounding the complex of ERαLBD, EST and a water molecule (PDB-ID: 1GWR) with the thickness of more than 10 Å from the protein surface) was imposed and the particle mesh Ewald method with the cutoff of 10.1 Å was used. Temperature regulation in the MD simulation was based on the Langevin dynamics with the damping constant $0.1ps^{-1}$. Structural optimizations were carried out through the following two stages: First, 2500 steps of optimization only for added hydrogen atoms were performed. Next, we carried out 2500 steps of optimization with restraint on heavy atoms by applying 0.5 kcal/(mol·Å) harmonic potential. These optimizations were executed until the total energy of protein converged. Then the temperature control and the pressure adjustment were performed sequentially. The system was relaxed by the MD in the NTV ensemble with 310K (MD time: 90 ps), and after that, relaxed by MD with the NTP ensemble until the average densities were well equilibrated (MD time: 50ps). After the temperature and pressure adjustments, 2 ns MD simulation was performed in NTV ensemble.

Configurations of ERαLBD, EST and a water molecule complex *in vacuo* and immersed with a 4 Å thick water were calculated by the FMO method at the MP2 level with the 6-31G* basis set. The configurations were obtained from a snapshot of 2 ns MD simulation (Figure S1). The ERαLBD consists of 244 residues (residue nos. 306-549) and has total charges of -6*e*.

Effect of Explicit Solvation.

We analyzed IFIEs and Mulliken atomic charges obtained from the FMO calculations at the MP2/6-31G* level and visualized ESPs calculated at the HF/6-31G* level for both the configurations of 2 ns MD snapshot *in vacuo* and in explicitly solvated water (Figure S1). The summations of these IFIEs (IFIE-sums) over all residues of H12 (residue nos. 536-546 (H12-all)) were calculated for configurations *in vacuo* and within explicit water molecules. The IFIE-sums of H12-all, H12-anionic residues and H12-neutral residues are listed in Table S1 and IFIE-sums of H12-anionic residues are shown in Figure S2. The differences in IFIE-sums of H12-anionic residues between *in vacuo* and in solvent water are less than 1.0 kcal/mol and those of H12-neutral residues between *in vacuo* and in solvent water are less than 6.0 kcal/mol. It is clear that IFIE is insensitive to solvent effect for explicit water model, especially concerning interactions between charged fragment pair.

The absence or presence of explicit solvent water has no remarkable effect on bare IFIE, but Mulliken charges show the changes in the atomic charges of complex [1]. The ERαLBD-EST complex *in vacuo* has total charge of -6*e*. On the other hand, the total charge of the complex becomes -2.31*e* and the atomic charges of -3.68*e* move to water molecules from the complex. Consequently, the ESPs of ERαLBD-ligand complex are affected by the CTs from protein to water molecules (See Figure 9 in the main article). The fragment charges of ERα in *vacuo* and in explicit water model are shown in Figure S3. The magnitude of negative charge values are markedly decreased in solvent water model; consequently, charge transfer occurs between protein and water molecules. The fragment charges of the negatively and positively charged residues are reduced by ca. 0.15*e* and 0.08*e*, respectively. Since amount of the fragment charge, which determines the character of each amino acid residue, is almost unchanged, we consider that the IFIE values would be unaffected by the explicit water molecules with the CTs.

On the other hand, the bare IFIE values generally tend to overestimate the electrostatic interactions between electrically charged fragment pair. For example, IFIE-sums of H12 with charged residues are shown to be as large as ca. 100 kcal/mol. To estimate interaction energies incorporating screening effect in the FMO method, analysis of the statistically corrected IFIE (SCIFIE) [2] is useful. The SCIFIE-sum of H12 with each charged residue is reduced by ca. 20% as compared to the IFIE-sum in Table S2.

Effect of Implicit Solvation.

In addition, we investigated the effect of implicit solvation models such as polarizable continuous model (PCM) [3] or Poisson-Boltzmann (PB) based model [4]. We performed the FMO calculations at the MP2/6-31G level with implicit solvent model based on the PB equation for 125-residue model of ERαLBD complexed with the ligand. (Figure S2) The model system consists of H12, key residues (Lys362, Asp351, Glu380, Lyss529), a ligand (EST or OHT), a water molecule and surrounding residues of those (residue nos. 338-430 and 516-547). Here, the IFIEs in solvation can be evaluated with or without solvent screening by induced surface charges around the fragment pair [3]. The IFIE with solvent screening is electrostatically reduced as compared to that without solvent screening, which is not so different from the IFIE obtained *in vacuo*, as seen in Table S3. For example, in the agonist-bound state (ERαLBD-EST complex), IFIE-sum of Lys529 with solvent screening is reduced by ca. 20% as compared to that without solvent screening. However, the behaviors of IFIEs with solvent screening are in quantitative agreement with those without solvent screening. Thus, we have concluded that the importance of the key residues (e.g. Lys362 and Lys529) is unchanged irrespective of the absence or presence of solvent.

Table S1. IFIEs of Residues in the H12 with Residues in Other Part of ERα in ERαLBD-EST (Agonist) Complex *in Vacuo* and in Solvated Water.

IFIE-sums of H12 (kcal/mol)	Condition	Fragment of ER-main in ERαLBD-EST complex						
		Asn348	**Asp351**	*Lys362*	**Glu380**	Trp383	*Lys529*	EST548
[a]12-all residues	*in vacuo*	-1.19	59.37	-52.39	92.68	-34.76	-121.40	0.19
	in solvent	-1.36	56.54	-52.77	95.92	-31.52	-114.84	-0.06
	Diff.	-0.17	-2.83	-0.38	3.24	3.24	6.56	-0.24
[b]H12-anionic residues	*in vacuo*	0.70	82.54	-52.14	86.30	-5.30	-122.08	0.26
	in solvent	0.77	81.71	-52.32	86.27	-4.29	-122.24	0.40
	Diff.	0.07	-0.83	-0.19	-0.02	1.01	-0.15	0.14
[c]H12-neutral residues	*in vacuo*	-1.89	-23.17	-0.26	6.38	-29.46	0.69	-0.07
	in solvent	-2.13	-25.17	-0.45	9.65	-27.23	7.40	-0.45
	Diff.	-0.24	-2.00	-0.19	3.26	2.23	6.71	-0.38

IFIEs between each ER-H12 residue and each ER-main residue were obtained from the FMO calculations at the MP2/6-31G* level. The summations of the IFIEs (IFIE-sums) were also calculated over all (H12-all), three anionic (H12-anionic), and eight neutral (H12-neutral) residues of H12. Anionic and cationic residues are indicated in bold and italic characters, respectively. [a] IFIE-sums between the H12-all residues (residue nos. 536-546) and each other residue. [b] IFIE-sums between the H12-anionic residues (Asp536, Glu542, and Asp545) and each other residue. [c] IFIE-sums between the H12-neutral residues (other residues except for the H12-anionic residues among the H12-all residues) and each other residue.

Table S2. IFIEs and SCIFIEs of Residues in the H12 with Residues in Other Part of ERα in ERαLBD-EST (agonist) Complex Using the 2 ns MD Snapshot *in Vacuo*.

Summation of interaction energies over H12 (kcal/mol)		Fragment of ER-main in ERaLBD-EST complex						
		Asn348	**Asp351**	*Lys362*	**Glu380**	Trp383	*Lys529*	EST548
[a]H12-all residues	IFIE	-1.19	59.37	-52.39	92.68	-34.76	-121.40	0.29
	SCIFIE	-1.94	37.64	-32.81	64.79	-32.80	-95.17	0.84
	Diff.	-0.74	-21.73	19.58	-27.89	1.96	26.23	0.55
[b]H12-anionic residues	IFIE	0.70	82.54	-52.14	86.30	-5.30	-122.08	0.26
	SCIFIE	-0.06	59.57	-31.50	58.71	-3.27	-94.53	0.87
	Diff.	-0.76	-22.97	20.64	-27.59	2.03	27.56	0.61
[c]H12-neutral residues	IFIE	-1.89	-23.17	-0.26	6.38	-29.46	0.69	0.03
	SCIFIE	-1.88	-21.93	-1.32	6.08	-29.53	-0.64	-0.03
	Diff.	0.01	1.24	-1.06	-0.30	-0.07	-1.33	-0.06

IFIEs between each ER-H12 residue and each ER-main residue were obtained from the FMO calculations at the MP2/6-31G* level. SCIFIEs were evaluated by using the IFIEs at the MP2/6-31G* level. Anionic and cationic residues are indicated in bold and italic characters, respectively. [a] IFIE-sums between the H12-all residues (residue nos. 536-546) and each other residue. [b] IFIE-sums between the H12-anionic residues (Asp536, Glu542, and Asp545) and each other residue. [c] IFIE-sums between the H12-neutral residues (other residues except for the H12-anionic residues among the H12-all residues) and each other residue.

Table S3. IFIEs of Residues in the H12 with Residues in Other Part of ERα ERαLBD-EST (Agonist) Complex in 125-residues Model System Calculated by the FMO method (*in Vacuo*) and the FMO-PB Method (in Solvent with or without Solvent Screening).

IFIE-sums of H12-all residues (kcal/mol)	Condition	Asn348	**Asp351**	*Lys362*	**Glu380**	Trp383	*Lys529*	Ligand
ERαLBD-EST complex	*in vacuo*	-16.27	37.13	-56.62	111.63	-23.38	-140.42	-0.09
	in solvent without screening	-15.49	37.88	-56.63	113.34	-22.93	-139.21	0.02
	in solvent with screening	-15.51	22.65	-44.62	92.89	-22.30	-116.05	0.16
ERαLBD-OHT complex	*in vacuo*	2.08	55.73	-168.08	16.02	-1.98	-36.57	-2.04
	in solvent without screening	2.04	54.77	-166.54	16.63	-2.05	-35.95	-1.88
	in solvent with screening	3.33	47.83	-149.26	10.25	-1.77	-29.61	-1.89

IFIEs between each ER-H12 residue and each ER-main residue were obtained from the FMO calculations at the MP2/6-31G level. The summations of the IFIEs (IFIE-sums) were also calculated over all (H12-all) residues of H12. Anionic and cationic residues are indicated in bold and italic characters, respectively.

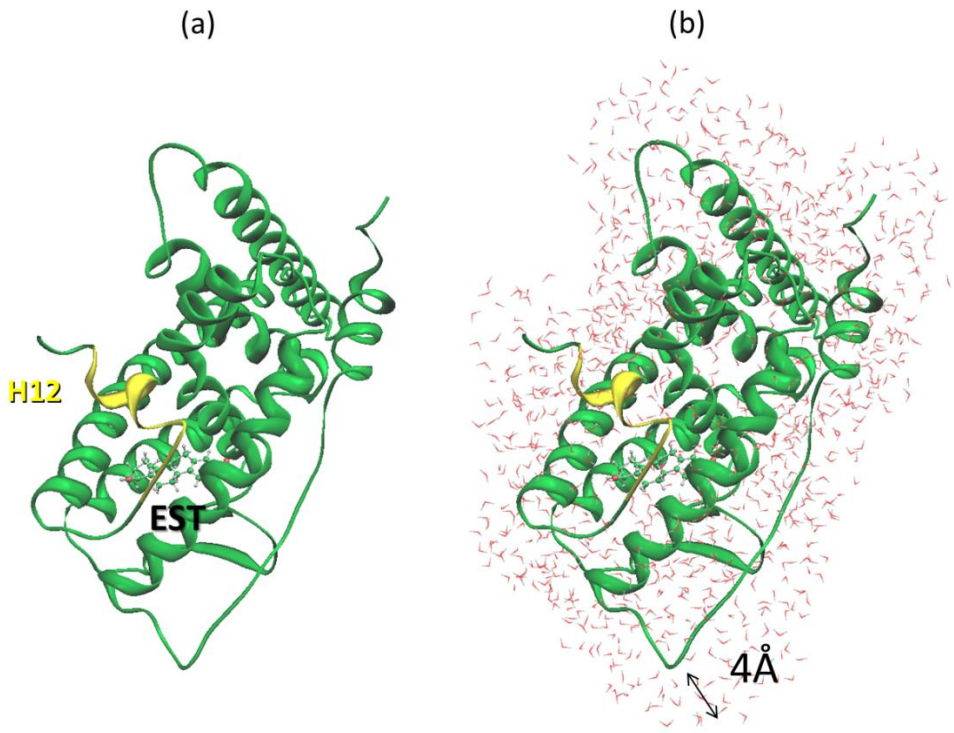

Figure S1 Configurations of ERαLBD-EST complex from MD snapshot at 2 ns ((a) *in vacuo* and (b) in explicit water model). Atoms of the ligand molecules and a water molecule are represented by ball and stick models, and H12 parts are in yellow and the other part ERαLBD are depicted in green.

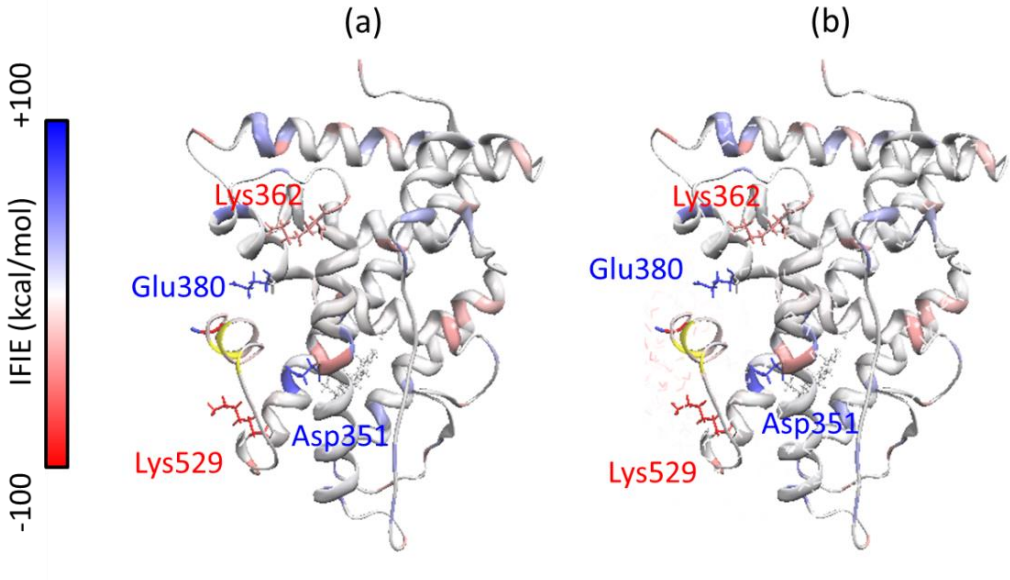

Figure S2 Visualizations of the summations of IFIEs (IFIE-sums) between the H12-anionic residues (Asp538, Glu542 and Asp545) and each other residue, for ERαLBD-EST complex *in vacuo* (a) and in the explicit solvent model (b). The IFIE-sums are shown with colors indicating attractive (red) and repulsive (blue) interactions. The H12-anionic residues are colored yellow in each figure.

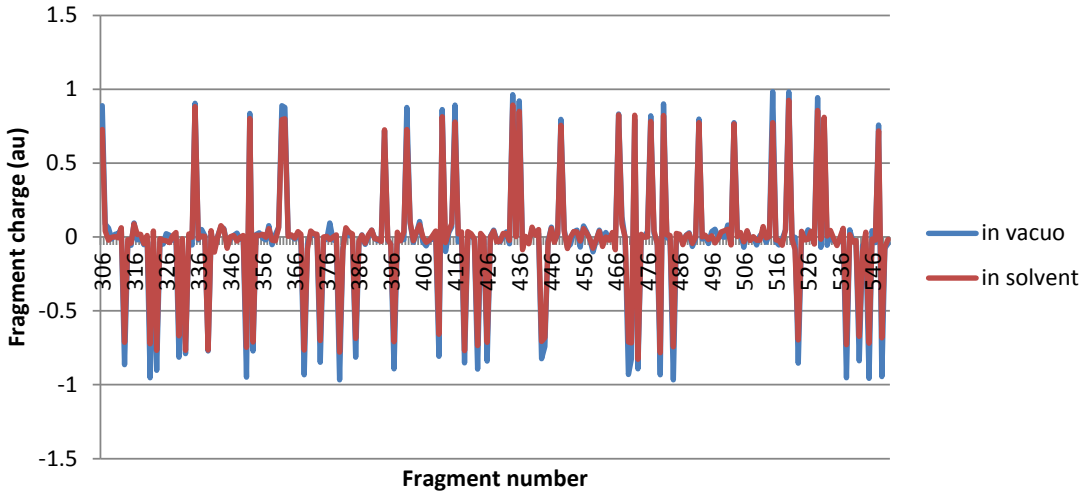

Figure S3 The Mulliken fragment charge q_i of ERαLBD-EST complex *in vacuo* and the explicit solvated water calculated by the FMO-MP2/6-31G* method The fragment charges *in vacuo* and the explicit solvated water are represented by blue and red lines, respectively.

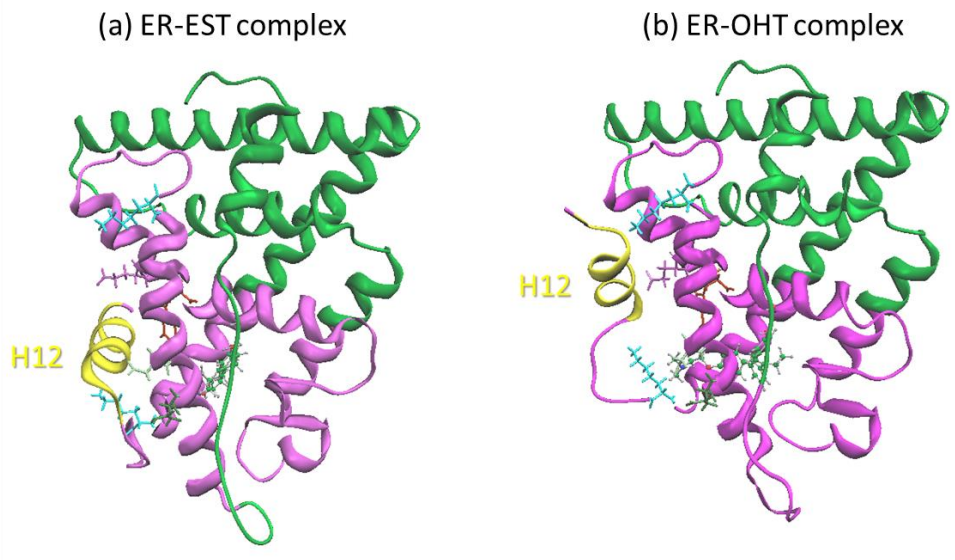

Figure S4 Model system for (a) the ERαLBD-EST (agonist) complex, and (b) the ERαLBD-OHT (antagonist) complex. In (a) and (b), atoms of the ligand molecules and a water molecule are represented by ball and stick models, atoms of the key residues (Lys362, Asp351, Glu380, Lyss529) are illustrated by stick. The model system structures of ERαLBD are depicted in pink, while the H12 parts are in yellow and the other part ERαLBD are depicted in green.

B. Comparing between Mulliken Atomic Charges and Natural Population Atomic Charges

We calculated fragment charges for Mulliken atomic charges and natural population atomic (NPA) net charges for model system (Figure S4). We carried out the FMO calculations at the MP2 level with the 6-31G basis set for the model system and analyzed fragment charges. The fragment charges for Mullieken atomic charges and NPA net charges are listed in Table S4. These charge differences are less than ca 0.1*e*. It is clear that fragment charges of Mulliken atomic charges did not change qualitatively those of NPA net charges [5, 6] for the model system.

Table S4. Fragment Charge Analyses for Mulliken Atomic Charges and NPA Atomic Net Charges for the Model System of ERαLBD Complexed with the Ligand and a Water Molecule.

	Fragment charge (au)		
	ERαLBD-EST complex		
	Mulliken	NPA	Diff.
Asn348	0.00	0.04	0.03
Asp351	-0.86	-0.95	-0.08
Lys362	0.93	0.98	0.04
Glu380	-0.87	-0.96	-0.09
Trp383	0.05	0.01	-0.04
Lys529	0.94	0.99	0.04
Leu536	0.01	-0.04	-0.05
Tyr537	0.04	0.03	-0.01
Asp538	-0.89	-0.94	-0.05
Leu539	0.02	0.02	0.00
Leu540	-0.01	-0.02	0.00
Leu541	-0.08	-0.04	0.04
Glu542	-0.94	-0.96	-0.02
Met543	-0.01	-0.02	-0.01
Leu544	-0.09	-0.06	0.04
Asp545	-0.93	-0.98	-0.05
Ala546	-0.08	-0.01	0.06
EST	-0.15	-0.16	-0.01
H12-all residues	-2.95	-3.00	-0.05

	ERαLBD-OHT complex		
	Mulliken	NPA	Diff.
Asn348	0.01	0.03	0.02
Asp351	-0.89	-0.95	-0.06
Lys362	0.89	0.95	0.06
Glu380	-0.94	-0.97	-0.03
Trp383	0.01	0.00	-0.01
Lys529	0.96	0.99	0.03
Leu536	0.05	0.01	-0.04
Tyr537	0.01	0.02	0.01
Asp538	-0.84	-0.94	-0.10
Leu539	-0.04	0.01	0.05
Leu540	0.00	-0.02	-0.02
Leu541	-0.01	0.00	0.00
Glu542	-0.94	-0.95	-0.02
Met543	-0.06	-0.02	0.04
Leu544	-0.10	-0.07	0.04
Asp545	-0.97	-0.99	-0.02
Ala546	-0.06	-0.02	0.04
OHT	-0.12	-0.12	0.00
H12-all residues	-2.96	-2.97	-0.01

C. Force Field Parameter of EST

We described force field parameter files for 17β-estradiol (EST).

Frcmod file for 17β-estradiol (EST)

```
remark goes here
MASS

BOND

ANGLE

DIHE

IMPROPER
ca-ca-ca-ha              1.1             180.0           2.0             General improper
torsional angle (2 general atom types)
ca-ca-ca-oh              1.1             180.0           2.0             Using default value

NONBON
```

Prep file for 17β-estradiol (EST)

```
    0      0      2

This is a remark line
molecule.res
EST     XYZ   0
CHANGE       OMIT DU     BEG
  0.0000
   1   DUMM   DU      M          999.000       999.0        -999.0              .00000
   2   DUMM   DU      M          999.000      -999.0         999.0              .00000
   3   DUMM   DU      M         -999.000       999.0         999.0              .00000
   4   C1     ca      M           -7.587000    -4.290000    15.607000    -0.179494
   5   C10    ca      E           -7.001000    -4.654000    14.354000    -0.167802
   6   H1     ha      E           -8.668000    -4.176000    15.691000     0.155805
   7   C2     ca      M           -6.772000    -4.081000    16.724000    -0.312196
```

8	H2	ha	E	-7.227000	-3.805000	17.675000	0.192855
9	C3	ca	M	-5.418000	-4.217000	16.643000	0.514213
10	O3	oh	S	-4.577000	-4.010000	17.752000	-0.660904
11	H3	ho	E	-3.538000	-4.124000	17.652000	0.453725
12	C4	ca	M	-4.794000	-4.580000	15.431000	-0.513459
13	H4	ha	E	-3.712000	-4.698000	15.368000	0.176428
14	C5	ca	M	-5.609000	-4.784000	14.313000	0.173612
15	C6	c3	M	-4.861000	-5.087000	13.021000	-0.023666
16	H5	hc	E	-4.336000	-4.185000	12.707000	0.037110
17	H6	hc	E	-4.138000	-5.879000	13.218000	0.037110
18	C7	c3	M	-5.766000	-5.534000	11.891000	-0.157026
19	H7	hc	E	-5.238000	-5.433000	10.943000	0.047841
20	H8	hc	E	-6.045000	-6.577000	12.042000	0.047841
21	C8	c3	M	-7.027000	-4.669000	11.865000	0.013271
22	H9	hc	E	-6.769000	-3.617000	11.747000	0.020288
23	C9	c3	M	-7.839000	-4.885000	13.140000	0.157149
24	H10	hc	E	-8.126000	-5.937000	13.154000	0.009742
25	C11	c3	M	-9.142000	-4.074000	13.044000	-0.059540
26	H11	hc	E	-9.718000	-4.192000	13.962000	0.033600
27	H12	hc	E	-8.909000	-3.020000	12.894000	0.033600
28	C12	c3	M	-9.960000	-4.607000	11.840000	-0.236899
29	H13	hc	E	-10.153000	-5.672000	11.970000	0.041795
30	H14	hc	E	-10.907000	-4.071000	11.775000	0.041795
31	C13	c3	M	-9.152000	-4.383000	10.558000	0.296478
32	C18	c3	3	-8.985000	-2.933000	10.167000	-0.366911
33	H22	hc	E	-8.401000	-2.869000	9.249000	0.088158
34	H23	hc	E	-8.468000	-2.398000	10.964000	0.088158
35	H24	hc	E	-9.965000	-2.484000	10.005000	0.088158
36	C14	c3	M	-7.814000	-5.154000	10.688000	0.057478
37	H15	hc	E	-8.020000	-6.218000	10.805000	-0.024975
38	C15	c3	M	-7.216000	-4.903000	9.300000	-0.227165
39	H16	hc	E	-6.936000	-3.858000	9.168000	0.069318
40	H17	hc	E	-6.349000	-5.538000	9.117000	0.069318
41	C16	c3	M	-8.419000	-5.295000	8.382000	-0.173305
42	H18	hc	E	-8.465000	-4.649000	7.505000	0.081071
43	H19	hc	E	-8.342000	-6.335000	8.064000	0.081071

```
  44  C17   c3    M          -9.667000   -5.084000    9.293000    0.321300
  45  H20   h1    E         -10.017000   -6.072000    9.593000   -0.029299
  46  O17   oh    M         -10.749000   -4.436000    8.639000   -0.711944
  47  H21   ho    E         -11.566000   -4.368000    9.296000    0.416296


LOOP
   C5  C10
   C9  C10
  C14   C8
  C17  C13

IMPROPER
  C10   C2   C1   H1
   C9   C5  C10   C1
   C1   C3   C2   H2
   C4   C2   C3   O3
   C5   C3   C4   H4
   C6   C4   C5  C10

DONE
STOP
```

D. Force Field Parameter of OHT

We described force field parameter files for 4-hydroxitamoxifen (OHT).

Frcmod file for 4-hydroxitamoxifen (OHT)

```
remark goes here
MASS

BOND

ANGLE
c3-c2-ca     63.001        117.200     Calculated with empirical approach

DIHE

IMPROPER
c2-c3-c2-ca              1.1             180.0           2.0             Using default value
ca-ca-ca-ha              1.1             180.0           2.0             General improper
torsional angle (2 general atom types)
c2-ca-c2-ca              1.1             180.0           2.0             Using default value
ca-ca-ca-oh              1.1             180.0           2.0             Using default value
ca-ca-ca-os              1.1             180.0           2.0             Using default value

NONBON
```

Prep file for 4-hydroxitamoxifen (OHT)

```
    0      0      2

This is a remark line
molecule.res
OHT     XYZ   0
CHANGE        OMIT DU     BEG
  0.0000
    1   DUMM   DU      M           999.000        999.0        -999.0              .00000
    2   DUMM   DU      M           999.000       -999.0         999.0              .00000
    3   DUMM   DU      M          -999.000        999.0         999.0              .00000
```

4	C10	c3	M	30.574000	1.465000	29.550000	-0.162862
5	H1	hc	E	30.094000	1.677000	30.505000	0.046250
6	H2	hc	E	29.970000	1.878000	28.742000	0.046250
7	H3	hc	E	31.564000	1.920000	29.532000	0.046250
8	C9	c3	M	30.702000	-0.023000	29.372000	-0.161767
9	H4	hc	E	31.301000	-0.424000	30.190000	0.091685
10	H5	hc	E	29.707000	-0.466000	29.399000	0.091685
11	C8	c2	M	31.363000	-0.388000	28.059000	-0.146849
12	C11	ca	S	32.788000	0.053000	27.962000	0.392251
13	C16	ca	B	33.241000	0.782000	26.842000	-0.217298
14	C15	ca	B	34.559000	1.235000	26.776000	-0.178635
15	C14	ca	B	35.451000	0.980000	27.799000	-0.138470
16	C13	ca	B	35.027000	0.270000	28.897000	-0.178635
17	C12	ca	S	33.707000	-0.188000	28.976000	-0.217298
18	H10	ha	E	33.391000	-0.748000	29.856000	0.132154
19	H9	ha	E	35.722000	0.063000	29.710000	0.150739
20	H8	ha	E	36.479000	1.337000	27.737000	0.138824
21	H7	ha	E	34.890000	1.799000	25.904000	0.150739
22	H6	ha	E	32.555000	0.993000	26.021000	0.132154
23	C7	c2	M	30.708000	-1.057000	27.065000	-0.091566
24	C1	ca	S	29.210000	-1.233000	27.016000	0.110738
25	C2	ca	B	28.609000	-2.490000	26.695000	-0.147904
26	C3	ca	B	27.215000	-2.613000	26.605000	-0.345610
27	C4	ca	B	26.409000	-1.482000	26.835000	0.423999
28	O4	oh	S	25.058000	-1.622000	26.722000	-0.555079
29	H13	ho	E	24.429000	-0.798000	26.887000	0.379696
30	C5	ca	B	26.992000	-0.235000	27.156000	-0.345610
31	C6	ca	S	28.375000	-0.134000	27.239000	-0.147904
32	H15	ha	E	28.822000	0.829000	27.485000	0.169006
33	H14	ha	E	26.364000	0.637000	27.336000	0.184819
34	H12	ha	E	26.761000	-3.573000	26.360000	0.184819
35	H11	ha	E	29.240000	-3.361000	26.519000	0.169006
36	C17	ca	M	31.411000	-1.690000	25.945000	-0.071297
37	C22	ca	B	30.966000	-1.528000	24.626000	-0.013565
38	C21	ca	S	31.601000	-2.135000	23.579000	-0.398791
39	H28	ha	E	31.237000	-1.992000	22.561000	0.179621

40	H29	ha	E	30.094000	-0.904000	24.431000	0.103253
41	C18	ca	M	32.529000	-2.496000	26.146000	-0.013565
42	H16	ha	E	32.897000	-2.639000	27.162000	0.103253
43	C19	ca	M	33.182000	-3.114000	25.117000	-0.398791
44	H17	ha	E	34.055000	-3.736000	25.315000	0.179621
45	C20	ca	M	32.725000	-2.944000	23.820000	0.487349
46	O20	os	M	33.296000	-3.554000	22.740000	-0.381563
47	C23	c3	M	32.900000	-3.183000	21.423000	0.219448
48	H18	h1	E	32.018000	-3.749000	21.122000	0.005244
49	H19	h1	E	32.679000	-2.116000	21.383000	0.005244
50	C24	c3	M	34.059000	-3.508000	20.520000	-0.031066
51	H20	h1	E	33.981000	-2.891000	19.625000	0.059941
52	H21	h1	E	34.983000	-3.269000	21.047000	0.059941
53	N24	n3	M	34.109000	-4.887000	20.118000	-0.261949
54	C26	c3	3	35.506000	-5.291000	19.922000	-0.232399
55	H25	h1	E	35.543000	-6.337000	19.617000	0.104482
56	H26	h1	E	36.055000	-5.165000	20.855000	0.104482
57	H27	h1	E	35.959000	-4.671000	19.148000	0.104482
58	C25	c3	M	33.390000	-5.111000	18.863000	-0.232399
59	H22	h1	E	33.450000	-6.165000	18.592000	0.104482
60	H23	h1	E	33.839000	-4.507000	18.074000	0.104482
61	H24	h1	E	32.345000	-4.828000	18.987000	0.104482

LOOP

C12	C11
C6	C1
C20	C21

IMPROPER

C7	C9	C8	C11
C8	C16	C11	C12
C11	C15	C16	H6
C16	C14	C15	H7
C15	C13	C14	H8
C14	C12	C13	H9

```
  C11   C13   C12   H10
   C8    C1    C7   C17
   C7    C2    C1    C6
   C1    C3    C2   H11
   C2    C4    C3   H12
   C3    C5    C4    O4
   C4    C6    C5   H14
   C1    C5    C6   H15
   C7   C22   C17   C18
  C17   C21   C22   H29
  C22   C20   C21   H28
  C17   C19   C18   H16
  C18   C20   C19   H17
  C21   C19   C20   O20

DONE
STOP
```

References

1. Komeiji, Y.; Ishida, T.; Fedorov, D. G.; Kitaura, K. Change in a Protein's Electronic Structure Induced by an Explicit Solvent: An Ab Initio Fragment Molecular Orbital Study of Ubiquitin. *J. Comput. Chem*. **2007**, *28*, 1750-1762.

2. Tanaka, S; Watanabe, C.; Okiyama, Y. Statistical Correction to Effective Interactions in the Fragment Molecular Orbital Method, *Chem. Phys. Lett.* **2013**, 556, 272-277.

3. Fedorov,D.G.; Kitaura, K. Energy Decomposition Analysis in Solution Based on the Fragment Molecular Orbital Method. *J. Phys. Chem.* A **2012**, *116*, 704–719.

4. Watanabe, H.; Okiyama, Y.; Nakano, T.; Tanaka, S. Incorporation of Solvation Effects into the Fragment Molecular Orbital Calculations with the Poisson-Boltzmann Equation, *Chem. Phys. Lett.* **2010**, *500*, 116-119.

5. Reed, A. E.; Weinhold, F. Natural bond orbital analysis of near-Hartree-Fock water dimer. *J. Chem. Phys.* **1983**, *78*, 4066-4073.

6. Reed, A. E.; Weinstock, R. B.; Weinhold, F. Natural population analysis. *J. Chem. Phys.* **1985**, *83*,735-746.